



PCCP

Imaging the Ordering of a Weakly Adsorbed Two-Dimensional Condensate: Ambient-Pressure Microscopy and Spectroscopy of CO₂ Molecules on Rutile TiO₂(110)

Journal:	<i>Physical Chemistry Chemical Physics</i>
Manuscript ID	CP-COM-03-2018-001614.R2
Article Type:	Communication
Date Submitted by the Author:	27-Apr-2018
Complete List of Authors:	<p>Hamlyn, Rebecca; Brookhaven National Laboratory, Chemistry Mahapatra, Mausumi; Brookhaven National Laboratory, Chemistry Grinter, David; Brookhaven National Laboratory Xu, Fang; Brookhaven National Laboratory, Chemistry Luo, Si ; Brookhaven National Laboratory, Chemistry Department Palomino, Robert; Brookhaven National Laboratory, Chemistry Department Kattel, Shyam; Brookhaven National Laboratory Waluyo, Iradwikanari; Brookhaven National Laboratory, National Synchrotron Light Source II Liu, Ping; Brookhaven National Lab, Chemistry Stacchiola, Dario; Brookhaven national Laboratory, Chemistry; Senanayake, Sanjaya; Brookhaven National Laboratory, Chemistry Rodriguez, Jose; Brookhaven National Laboratory, Chemistry Department</p>

SCHOLARONE™
Manuscripts

Imaging the Ordering of a Weakly Adsorbed Two-Dimensional Condensate: Ambient-Pressure Microscopy and Spectroscopy of CO₂ Molecules on Rutile TiO₂(110)

Rebecca C. E. Hamlyn^{†,§}, Mausumi Mahapatra[†], David C. Grinter^{†,§}, Fang Xu^{†,ψ}, Si Luo^{†,§}, Robert M. Palomino[†], Shyam Kattel[†], Iradwikanari Waluyo[‡], Ping Liu[†], Dario J. Stacchiola^{†,Δ}, Sanjaya D. Senanayake[†] and José A. Rodríguez^{*,†,§}

[†]Chemistry Department and [‡]National Synchrotron Light Source II, Brookhaven National Laboratory, Upton, New York 11973

[§]Department of Chemistry, Stony Brook University, Stony Brook, NY, 11794

Disorder-Order transitions in a weakly adsorbed two-dimensional film have been identified for the first time using ambient-pressure scanning tunneling microscopy (AP-STM) and X-ray photoelectron spectroscopy (AP-XPS). As of late, a great effort has been devoted to the capture, activation and conversion of carbon dioxide (CO₂), a ubiquitous greenhouse gas and by-product of many chemical processes. The high stability and non-polar nature of CO₂ leads to weak bonding with well-defined surfaces of metals and oxides. CO₂ adsorbs molecularly on the rutile TiO₂(110) surface with a low adsorption energy of ~ 10 kcal/mol. In spite of this weak binding, images of AP-STM show that a substantial amount of CO₂ can reside on a TiO₂(110) surface at room temperature forming two-dimensionally ordered films. We have employed microscopic imaging under *in situ* conditions, soft X-ray spectroscopy and theory to decipher the unique ordering behavior seen for CO₂ on TiO₂(110).

Order-disorder phenomena in two-dimensional films play a relevant role in many areas of chemistry, physics and materials science¹⁻⁴. An important question is why van der Waals gases such as CH₄, N₂, or CO₂ condense onto solid surfaces in monolayers instead of droplets of small crystallites^{1,4}. In the case of chemisorption, the bonding with a solid substrate can induce ordering in a film of a gas², modulated by interactions which impose the substrate periodicity upon the adsorbed film. Physisorbed systems, on the other hand, exhibit extremely weak interactions with the solid surface and should be a good approximation to a free-floating film or overlayer. However, in some cases ordering can be modulated by weak adsorption forces¹. Using ambient-pressure scanning tunneling microscopy (AP-STM) we have identified and imaged one of these unusual systems: CO₂ interacting with rutile TiO₂(110).

The chemistry at play in this system is of scientific and economic pertinence. CO₂ is often used as a probe molecule for the elucidation of surface area, basicity and defect sites⁵. Furthermore, activation of CO₂ followed by its catalytic conversion to value-added products can be a key process in enabling the utilization of an abundant feedstock with the concomitant benefit of atmospheric CO₂ reduction⁶⁻⁸. The adsorption of CO₂ on rutile TiO₂(110) has been studied using techniques such as temperature programmed desorption^{12,11}, vibrational spectroscopies^{5,11,13} and photoemission¹⁴ which show that CO₂ adsorbs molecularly on the surface with a low adsorption energy of 9-12 kcal/mol (0.4-0.5 eV)¹⁵. Low temperature scanning tunneling microscopy (STM) and complementary density functional theory (DFT) studies of CO₂ on TiO₂ have been reported in the literature with examination of the adsorbate on different surface sites¹⁶⁻¹⁸. To the best of our knowledge, all the previous STM studies were carried out at low temperatures under UHV conditions and no significant ordering was observed since a real two-dimensional condensate film could not be formed without exposure to a background gas.

Here, we report for the first time CO₂ adsorption on rutile TiO₂(110) at 300 K under an ambient pressure of CO₂. Images of STM for a TiO₂(110) surface exposed to 0.53 Torr of CO₂ are shown in Figure 1. The adsorbate structure is located along the Ti_{5c} rows. The molecules are detected as single symmetric protrusions at an apparent height of about 1.0 Å with respect to the Ti rows. They are stable over the timescale of several minutes, with some minor diffusion along the Ti_{5c} rows in the [001] direction. Within the first scans, the adsorbates are seen to develop a loose superstructure in some areas, occupying every-other unit cell along the titanium rows. Examples are annotated in Figure 1B & D. The coverage is variable over different regions, with some (1×3) and (1×4) arrangements corresponding to about 0.2 monolayer (ML; 1 ML is defined as one CO₂ molecule for each 5-

fold Ti atom in the $\text{TiO}_2(110)$ unit cell), (Figure 1B), and other regions that exhibit a coherent (1×2) superstructure (Figure 1D). The maximum coverage seen at 0.5 ML is attributed to these latter areas, giving an intermolecular distance of about 6.0 Å.

Despite diffusion along the Ti_{5c} rows, neighboring CO_2 molecules tend to avoid adjacent Ti_{5c} sites

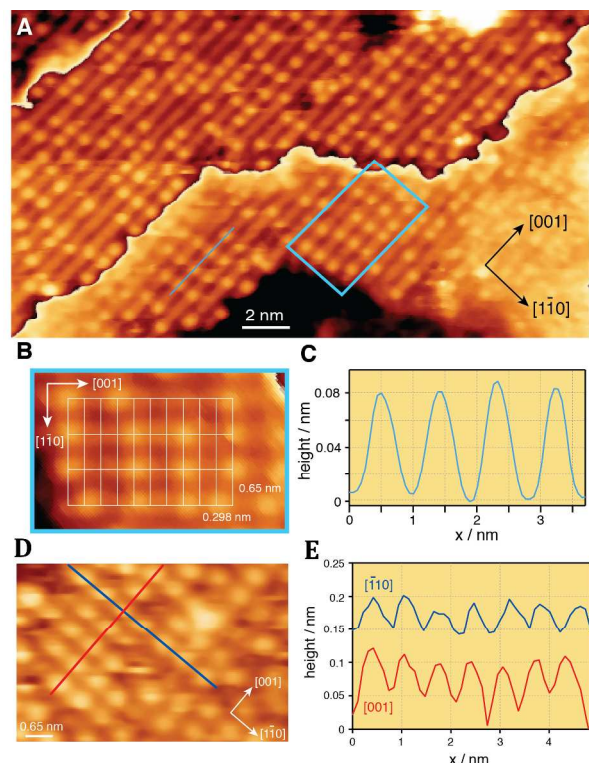


Fig. 1 A) STM image of the rutile $\text{TiO}_2(110)$ surface under 0.53 Torr CO_2 at 300 K. ($24 \times 14 \text{ nm}^2$, $V = +1.73 \text{ V}$, $I = 0.11 \text{ nA}$). Individual terrace contrast was adjusted independently for ease of viewing. B) & D) Small areas demonstrating the adsorbate spacing relative to the titania substrate. Image B, taken from the blue rectangle in 1A, includes an overlay of the rutile $\text{TiO}_2(110)$ unit cell. Image D depicts the presence of (1×2) domains of adsorbates on the titania surface. ($6.5 \times 4.3 \text{ nm}^2$, $V = +1.73 \text{ V}$, $I = 0.07 \text{ nA}$). C) Line profile from image A. E) Line profiles from image D.

(though these do occur on occasion). Under these conditions, there is no aggregation of CO_2 into islands but rather a distributed wetting of the surface to form a 2-D condensate or film. Upon evacuation of the background gas, CO_2 on the Ti_{5c} rows desorbs from the surface.

We have followed this interaction as a function of time and gas exposure, see Figure 2. Films of the adsorbate are always present on the rutile $\text{TiO}_2(110)$ surface independently of the pressures investigated and the time of exposure. In all the terraces of the titania substrate one can see a large population of CO_2 molecules. In the images, it is difficult to quantify the total amount of adsorbed CO_2 but it is clear that the CO_2 was only adsorbed on Ti_{5c} sites. Saturation of surface sites occurs quickly and the relative order of the film with respect to the substrate does not change with increased exposure. A good number of the adsorbed CO_2 molecules remain at a constant position but the total population of the adsorbate on a particular row of Ti_{5c} can change with time. Figure 3 shows a close-up of a section of the surface as function of time. The curves in the right-side panel display height profiles for CO_2 molecules on a Ti_{5c} row

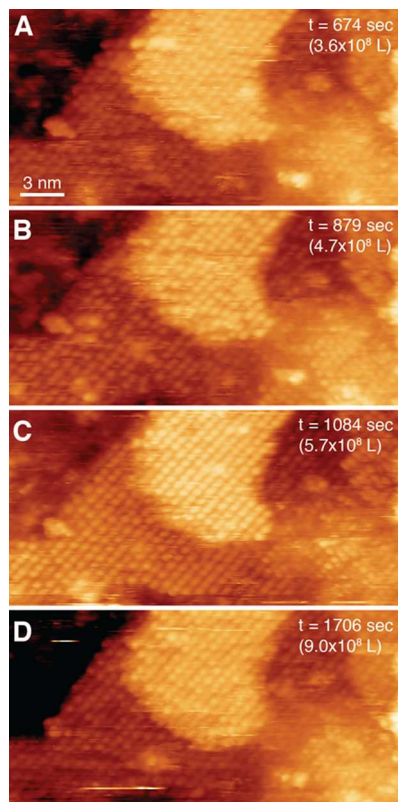


Fig. 2 STM images of the rutile $\text{TiO}_2(110)$ surface under 0.53 Torr CO_2 at 300 K showing the evolution of the surface with time. ($27 \times 13 \text{ nm}^2$, $V = +1.73 \text{ V}$, $I = 0.06 \text{ nA}$)

over time with increasing exposure as seen in Figure 2. The row of Ti_{5c} sites always has adsorbed CO_2 but some of the molecules move. This mobility is consistent with the low adsorption energy of CO_2 on the titania surface.¹⁵

Ambient-pressure XPS clarified important aspects of the interaction of CO_2 with rutile $\text{TiO}_2(110)$. In the Ti 2p region (Figure 4A), one can see strong features for Ti^{4+} and weak features for Ti^{3+} .^{14,19} The Ti^{3+} sites could be associated with O vacancies or with

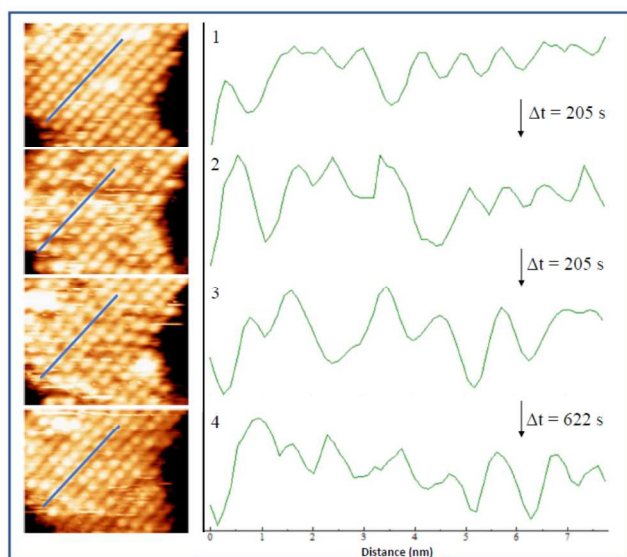


Fig. 3 Height profiles for CO_2 molecules on a Ti_{5c} row as a function of time with increasing CO_2 exposure as seen in Figure 2 ($V = +1.73 \text{ V}$, $I = 0.06 \text{ nA}$).

interstitial sites in the oxide lattice.^{14,19} In Figure 4A, the features for Ti^{3+} sites disappear as the pressure of CO_2 increases. This is consistent with the adsorption and dissociation of CO_2 on O vacancies of the surface. The

CO₂ decomposes into atomic O, filling vacancy sites, and CO, which desorbs into the gas phase. It is known that oxygen vacancies activate the dissociation of CO₂ on titania and other oxide surfaces.^{10,12,15,20,21,22} Thus, at the CO₂ pressures used for the STM experiments, the Ti³⁺ sites are removed and titania is close to fully oxidized. No carbonate species was detected in AP-XPS after the adsorption of CO₂ on the TiO₂(110) surface. The C 1s spectra in Figure 4B consist of two major peaks at 292 eV and 289.7 eV, which appear at a CO₂ gas pressure of 10⁻² Torr and grow with increasing pressures. The C 1s peak at 292 eV is due to CO₂ in the gas phase and the smaller peak at 289.7 eV corresponds to molecularly bound CO₂ on the surface. Upon evacuation of the gas from the chamber, the surface remains largely oxidized with no CO₂ adsorbed, as seen in the darkest spectrum in Figure 4A.

Thus, STM and XPS results show that at ambient pressures, CO₂ can be present on a TiO₂(110) surface even at 300 K. AP-XPS spectra indicate that CO₂ mostly adsorbs molecularly on the TiO₂(110) surface (Figure 4B) in agreement with previous low temperature XPS data¹⁸, but some of the CO₂ molecules interact with O_{vac} sites. Our experimental data show that at 300 K, as opposed to lower temperatures, a higher CO₂ pressure (10⁻² Torr or higher) is required for molecular adsorption on TiO₂(110), suggesting an equilibrium between the CO₂ gas and a two-dimensional (2-D) film on the surface.

DFT calculations were performed with the projector augmented wave method^{23,24} as implemented in the Vienna Ab-initio simulation package (VASP)²⁵⁻²⁷, using three different functionals (described in Supplemental Information, see also Table 1). Following previous theoretical and experimental studies,^{10,16-18,20} various configurations of CO₂ on Ti_{5c} rows

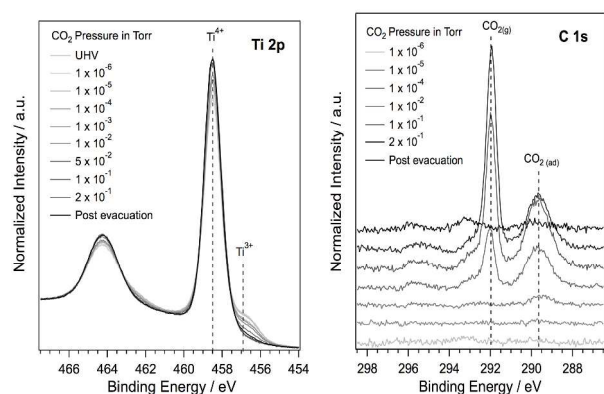


Fig. 4 AP-XPS spectra of rutile TiO₂(110) under increasing CO₂ pressures at 300 K including (A) the Ti 2p and (B) the C 1s regions.

were considered to explain the STM images (Fig S1). These included two different coverages: 0.125 ML (one CO₂ molecule on a 2×4 slab as shown in Fig S1) and 0.5 ML (4 CO₂ molecules on a 2×4 slab, the highest coverage observed experimentally) where the absolute coverage is referenced to the number of surface Ti_{5c} atoms. The low 0.125 ML coverage allowed us to elucidate the bonding geometry and adsorption energy without lateral interactions between molecules present in the high 0.5 ML coverage which eventually could drive the ordering of the overlayer. The adsorption geometry of the three most stable CO₂ configurations at 0.5 ML coverage and their corresponding STM simulated images are shown in Figure 5. In the first configuration (Figure 5a and d), CO₂ assumes a bidentate adsorption geometry parallel to the surface with each CO₂ oxygen atom bound to a Ti_{5c} atom along the <110> direction. The other two are monodentate adsorption conformations where each CO₂ is bound to a Ti site via one O atom, and differ in the orientation of the O=C=O bond axis. The adsorption energies of the three different configurations of CO₂ at 0.125 and 0.5 ML coverages are reported in Table 1. PW91 and PBE functionals yield similar adsorption energies while the PBE+TSvdw functional combination shows stronger binding due to the addition of van der Waals interactions. At ~ 0.5 eV (11.5 kcal/mol), the binding energy obtained by using the PBE+TSvdw combination is consistent with values reported in experimental studies^{12,15,28}.

The adsorption energy of CO₂ slightly decreases (0.01-0.03 eV) with an increase in coverage which suggests slight lateral repulsive interactions between molecules at higher coverages. The energy difference between the three different geometries of adsorbed CO₂ is negligible and can be easily overcome at room temperature. Therefore, the adsorption geometry from an energetics standpoint is inconclusive. We performed STM

simulations of the DFT structures, and are shown in the bottom panel of Figure 5. The simulated image of a vertical CO_2

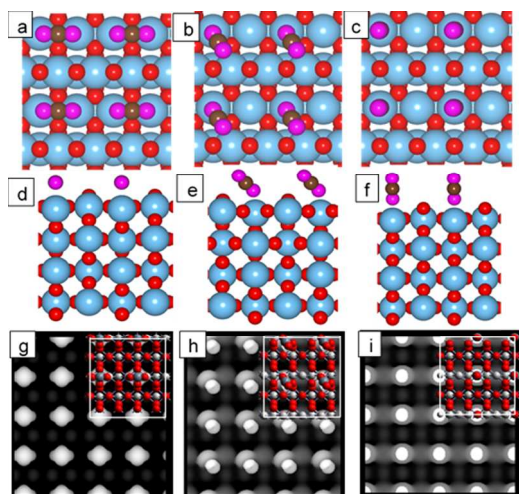


Fig. 5 Bird's eye (upper row) and side (middle row) views of the main adsorption configurations of 0.5 ML coverage of CO_2 on Ti_{5c} sites with corresponding STM simulated images in the bottom row. DFT optimized structures of the flat-lying, tilted and vertical CO_2 are shown in (a, d), (b, e) and (c, f), respectively. The lattice colors are cyan for Ti and red for O atoms, with brown for C and magenta for O atoms of the adsorbed CO_2 molecules. The STM simulated images of flat-lying, tilted and vertical CO_2 are shown in (g), (h) and (i), respectively, where the unit cell used for the calculation is also shown in the overlay.

CO_2 geometry	Adsorption Energy (eV)					
	PW91		PBE		PBE+TSvdw	
Functional						
Coverage (ML):	0.125	0.5	0.125	0.5	0.125	0.5
flat-lying	-0.18	-0.17	-0.15	-0.14	-0.51	-0.50
tilted	-0.28	-0.27	-0.26	-0.25	-0.56	-0.55
upright	-0.25	-0.22	-0.23	-0.20	-0.49	-0.46

Table 1. Adsorption energies of 0.125 and 0.5 ML of CO_2 on rutile $\text{TiO}_2(110)$ for various conformations and DFT functionals

(Figure 5i) is the best match for the experimentally observed STM images, wherein the underlying rutile row structure is still visible (see full analysis in Figures S2-S5). Previous results for the adsorption of isolated molecules of CO_2 at low temperature (80-180 K) under UHV also suggest that a monodentate orientation normal to the surface plane is the most likely bonding conformation^{18,20,28}.

For the ordering of an adsorbate, an important factor to consider involves the bonding forces between the adsorbate and substrate, which can be balanced by lateral interactions between molecules in the adsorbed film². The electronic effect after CO_2 adsorption on TiO_2 was characterized by charge density difference (CDD) plots as shown in Figure 6. The CDD plots suggest that upon adsorption, the CO_2

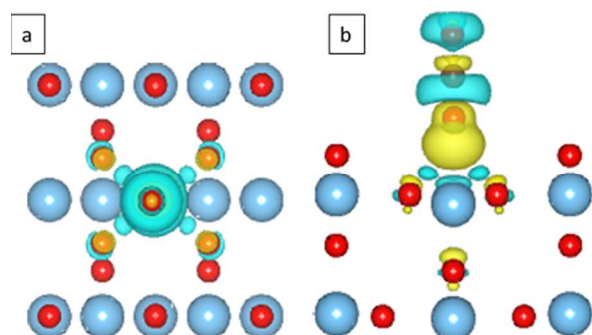


Fig. 6 Calculated charge density difference for CO₂ adsorbed on rutile TiO₂ (110). a) Vertical CO₂ adsorption bird's eye view and b) side view. The isosurface level was chosen as 0.001e/Å³. Contours indicate the electron density increases (yellow) or decreases (cyan) by 0.001 electrons/Å³.

molecule is slightly polarized and perturbs surface states of the substrate. This minor perturbation in the surface states of TiO₂(110) induced by CO₂ adsorption could contribute to ordering of the CO₂ film. In any case, since lateral interactions are negligible (Table 1), the main cause for the ordering arises from weak adsorption forces between the molecule and titania.

In summary, in this study we have shown that, in spite of weak binding, a substantial amount of CO₂ can reside on a TiO₂(110) surface at room temperature forming two-dimensionally ordered films. This phenomenon may occur on other oxides and must be taken into consideration when dealing with catalytic or photochemical processes aimed at the conversion or destruction of CO₂.

Electronic Supplementary Information (ESI)

Supplementary information includes a more detailed discussion of the experimental methods and theoretical studies (Figures S1 – S5).

Author Information

Corresponding Author

Email: rodriguez@bnl.gov, Bldg. 555A, Brookhaven National Lab, P.O. Box 5000, Upton, NY 11973-5000

Present Addresses

[§]Surfaces and Interfaces, Diamond Light Source, Didcot, Oxfordshire, United Kingdom OX11 0DE

^ψDepartment of Chemistry and Chemical Biology, Harvard University, Cambridge, MA 02138

^δChemical Science Division, Oak Ridge National Laboratory, Oak Ridge, TN 37831

^ΔCenter for Functional Nanomaterials, Brookhaven National Laboratory, Upton, NY 11973

Conflict of interest

There are no conflicts to declare.

Acknowledgements

The research carried out at Brookhaven National Laboratory, was supported by the U.S. Department of Energy, Office of Science and Office of Basic Energy Sciences, Division of Chemical Sciences, Biosciences, and Geoscience, under contract No. DE-SC0012704. This work utilized instrumentation and computational resources of the Center for Functional Nanomaterials and the 23-ID-2 beamline at the National Synchrotron Light Source II (IOS), which are D.O.E. Office of Science User Facilities. SDS is supported by a D. O. E. Early Career Award.

Notes and References

- (1) R. Marx, *Phys. Rep.* 1985, **125**, 1-67.
- (2) M.A. Van Hove, W.H. Weinberg and C.M. Chan, Two-Dimensional Order-Disorder Phase Transitions. In: *Low-Energy Electron Diffraction*. Springer Series in Surface Science. Berlin, Heidelberg, 1986; pp 318–377.
- (3) J. Lu, K. Zhang, X.F. Liu, H. Zhang, T.C. Sum, A.H. Castro Neto and K.P. Loh, *Nat. Commun.* 2013, **4**, [dx.doi.org/10.1038/ncomms2401](https://doi.org/10.1038/ncomms2401).

- (4) S. Piccinin and C. Stampfl, *Phys. Rev. B*, 2010, **81**, 111427.
 - (5) G. Ramis, G. Busca and V. Lorenzelli, *Mater. Chem. Phys.* 1991, **29**, 425-435.
 - (6) M. Aresta, *Carbon dioxide as chemical feedstock*; John Wiley & Sons Ltd., 2008.
 - (7) A. Baiker, *Applied Organometallic Chemistry*, 2000, **14**, 751-762.
 - (8) L. Marini, *Geological Sequestration of Carbon Dioxide: Thermodynamics, Kinetics, and Reaction Path Modeling*; Elsevier, 2006.
 - (9) Q. Pan, B.H. Liu, M.E. McBriarty, Y. Martynova, I.M.N. Groot, S. Wang, M.J. Bedzyk, S. Shaikhutdinov and H.-J. Freund, *Catal. Letters* 2014, **144**, 648-655.
 - (10) H.-J. Freund and M.W. Roberts, *Surf. Sci. Rep.* 1996, **25**, 225-273.
 - (11) M.A. Henderson, *Surf. Sci.* 1996, **355**, 151-166.
 - (12) M.A. Henderson, *Surf. Sci.* 1998, **400**, 203-219.
 - (13) J. Raskó, *Catal. Letters* 1998, **56**, 11-18.
 - (14) K. Tanaka, K. Miyahara and I. Toyoshima, *J. Phys. Chem* 1984, **88**, 3504-3508.
 - (15) D.C. Sorescu, J. Lee, W.A. Al-Saidi, and K.D. Jordan, *J. Chem. Phys.* 2011, **134**, 104707.
 - (16) A. Markovits, A. Fahmi, and C. Minot, *J. Mol. Struct.* 1996, **371**, 219-230.
 - (17) J. Lee, D.C. Sorescu and X. Deng, *J. Am. Chem. Soc* 2011, **133**, 10066-10069.
 - (18) D.P. Acharya, N. Camillone, and P. Sutter, *J. Phys. Chem. C* 2011, **115**, 12095-12105.
 - (19) S. Wendt, P.T. Sprunger, E. Lira, G.K.H. Madsen, Z. Li, J.O. Hansen, J.O. Hansen, J. Matthiesen, A. Blekinge-Rasmussen, E. Laegsgaard, B. Hammer and F. Besenbacher, *Science*, 2008, **320**, 1755-1759.
 - (20) S. Huygh, A. Bogaerts, and E.C. Neyts, *J. Phys. Chem. C*, 2016, **120**, 21659-21669.
 - (21) T.L. Thompson, O. Diwald, and J.T. Yates, *J. Phys. B*, 2003, **107**, 11700-11704.
 - (22) Z. Liu, P. Lustemberg, R.A. Gutiérrez, J.J. Carey, R.M. Palomino, M. Vorokhta, D.C. Grinter, P.J. Ramirez, V. Matolín, M. Nolan, M.V. Ganduglia-Pirovano, S.D. Senanayake, and J.A. Rodriguez, *Angew. Chem. Int. Ed.* 2017, **56**, 13041-13046.
 - (23) G. Kresse and D. Joubert, *Phys. Rev. B* 1999, **59**, 1758-1775.
 - (24) P.E. Blöchl, *Phys. Rev. B* 1994, **50**, 17953-17979.
 - (25) G. Kresse and J. Hafner, *Phys. Rev. B* 1993, **47**, 558-561.
 - (26) G. Kresse and J. Furthmüller, *J. Phys. Rev. B* 1996, **54**, 11169-11175.
 - (27) G. Kresse and J. Furthmüller, *Comput. Mater. Sci.* 1996, **6**, 15-50.
 - (28) S. Funk, B. Hokkanen, E. Johnson and U. Burghaus, *Chem. Phys. Lett.* 2006, **422**, 461-465.
-